

1 Article

2 Paleoenvironment Variability during Termination I 3 at the Reykjanes Ridge, North Atlantic

4 Alexander Matul ^{1,*}, Max S. Barash ¹, Tatyana A. Khusid ¹, Padmasini Behera ², Manish Tiwari ²

5 ¹ Shirshov Institute of Oceanology, Nahimovskiy prospekt 36, 117997 Moscow, Russia; AM: amatul@mail.ru,
6 MSB: barashms@yandex.ru, TAK: tkhusid@mail.ru

7 ² National Centre for Antarctic and Ocean Research, Vasco-da-Gama, 403 804 Goa, India; PB:
8 pbehera@ncaor.gov.in; MT: manish@ncaor.gov.in

9 ***Correspondence:**

10 Alexander Matul, Shirshov Institute of Oceanology, Nahimovskiy prospekt 36, 117997 Moscow, Russia;
11 E-mail: amatul@mail.ru; Tel. +7-499-1292172

12

13 **Abstract:**

14 The micropaleontological study (radiolarians and foraminifera) of the sediment core AMK-340,
15 Reykjanes Ridge, North Atlantic, combined with the radiocarbon dating and Oxygen/Carbon
16 isotopic record, provided data for the reconstruction of the summer paleotemperature on the water
17 depth of 100 m, and paleoenvironments during the Termination I in the age interval of 14.5-8 ka. The
18 response of the main microfossil species on the paleoceanographic changes within the
19 Bølling-Allerød (BA) warming, the Younger Dryas (YD) cold event, and final transition to the warm
20 Holocene was different. The BA warming was well reflected in the radiolarian and benthic but not
21 planktic foraminiferal record. The high abundances of the cold-water radiolarian species
22 *Amphimelissa setosa* as the Greenland/Iceland Sea indicator marked a cooling at the end of the BA and
23 within the start of the YD at 13.2-12.3 ka. The micropaleontological and isotopic data together with
24 the paleotemperature estimates for the Reykjanes Ridge at 60°N document that, after the warm BA,
25 the middle YD ca. 12.5-12.2 ka was the next significant step toward the Holocene warming. Start of
26 the Holocene interglacial conditions was reflected in abundant occurrence of the microfossils being
27 indicators of the open boreal North Atlantic environments and lower oxygen isotope values
28 indicating increasing warmth.

29 **Keywords:** global warming and environmental change; Late Quaternary paleoenvironments;
30 Termination I; sea-water paleotemperature; marine microfossils; North Atlantic; stable isotopes

31

32 **1. Introduction**

33 Our study presents new results on the North Atlantic paleoceanography during the last
34 deglaciation which was time of the abrupt climatic changes (general warming superimposed by
35 sudden short glacial reversals). Climatic situation in the North Atlantic, through the Atlantic
36 thermohaline circulation or North Atlantic meridional overturning circulation (NAMOC), mediates
37 climate on the surrounding land, and climatic connections between hemispheres [1]. The sea surface
38 conditions in the North Atlantic significantly influence the major modes of regional atmospheric
39 circulation (meridional or zonal) [2] causing warming or cooling episodes. Rapid changes in the
40 NAMOC and on the North Atlantic surface during the last deglaciation could be strongly related to
41 the changes of the climatic conditions (global warming, melt-water discharge from land ice, sea-ice
42 distribution) [3]. Overpeck et al. (1998) [4] postulated an apparent synchronicity of the rapid climate
43 events in the circum-North Atlantic during the last deglaciation but called for new high-resolution
44 studies to prove this.

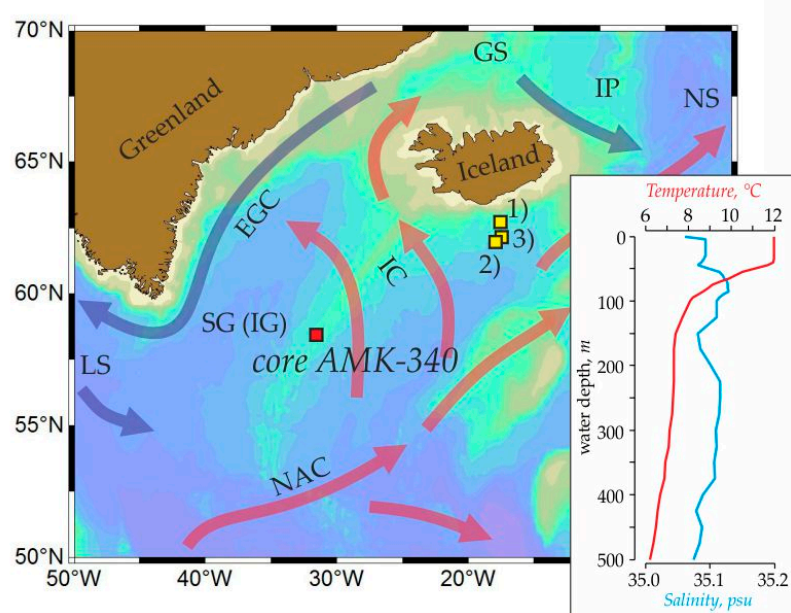
45 We use the micropaleontological data from the sediment core AMK-340, combined with the
46 radiocarbon dating of the absolute age and oxygen/carbon isotopic record, to estimate the sea
47 subsurface summer temperature and to describe the paleoenvironmental changes within the
48 Termination I on the Reykjanes Ridge, at ca. 60°N of the North Atlantic. Multiple publications on the
49 Late Quaternary paleoceanography of the subpolar to polar North Atlantic revealed main
50 characteristics of the climatic trends and variations during the last glacial cycle based on the
51 extensive analysis of the micropaleontology and paleotemperature reconstructions [5, and
52 references therein]. Our aim is to get an additional quantitative information on the local
53 paleoenvironments (sea subsurface temperature), and compare it with the global/regional
54 paleoclimatic archives. Working approach is a reconstruction of the paleotemperature based on the
55 factor analysis of the radiolarian and planktic foraminiferal data in the same samples of the sediment
56 core. The radiolarian distribution and paleotemperature estimates on the radiolarians (old
57 “graphical” paleotemperature method, and method of spline interpolations as a modification of the
58 Q-mode analysis) for the core AMK-340 was presented by Matul [6], and Matul and Yushina [7].
59 This paper uses a deeply reworked modern radiolarian database, corrected radiolarian data in the
60 core, newly constructed modern planktic foraminiferal database, a standard paleotemperature

61 method of the Q-mode analysis and transfer functions realized as a software PanTool Box [8], and
62 involves unpublished data on the planktic and benthic foraminifera in the core.

63 The study area is located on the eastern margin of the Subpolar (Irminger) Gyre. The western
64 branch of the Irminger Current, splitted from the warm North Atlantic Current, influences a modern
65 oceanographic situation on the Reykjanes Ridge [9]. Conversion of surface/deep warm/cold waters
66 of the Irminger Current, East Greenland Current, and Labrador Sea Water within the Irminger Gyre
67 is unstable exhibiting large interannual variability of the water flows on the sea surface and deeper
68 levels thus complicating the local features of the NAMOC [10]. The average summer sea surface
69 temperature in the location of the core AMK-340 is ca. 12°C [11]. At the end of the last glacial period,
70 before ca. 14 thousand years ago (ka), sea surface temperatures south of Iceland dropped down to
71 0-2°C [12], and we expect to get a picture of the prominent temperature and environmental changes
72 within the transition from the last glacial to the Holocene interglacial on the Reykjanes Ridge.

73 **2. Material and Methods**

74 The sediment gravity core AMK-340, 4th cruise of the Russian RV "Akademik Mstislav
75 Keldysh" in 1982, was obtained from the central area of the Reykjanes Ridge, North Atlantic
76 (58°30.6'N, 31°31.2'W; water depth of 1689 m; core length of 387 cm) (Figure 1). A general lithology
77 of the core is (1) 0 to 241 cm pelitic calcareous muds with CaCO₃ content of 40-50%, (2) 241 to 307 cm
78 pelitic weakly calcareous muds with CaCO₃ content of 10-25%, (3) 307 to 387 cm pelitic muds with
79 CaCO₃ content of ≈10% intermittent by the thin layers of the pelitic weakly siliceous muds.



80

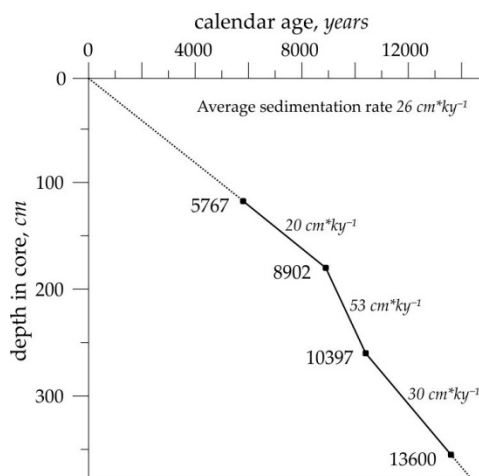
81 **Figure 1.** Core location (red square) and modern regional oceanographic conditions. Sediment cores (yellow
 82 squares) which were mentioned in the paleoceanographic interpretations: 1) RAPiD-10-1P, 62.9755°N,
 83 17.5895°W, 1237 m water depth; 2) RAPiD-12-1K, 62.09°N, 17.82°W, 1938 m water depth; 3) RAPiD-15-4P:
 84 62.293°N, 17.134°W, 2133 m water depth [13-14]. Vertical summer salinity/temperature profiles are extracted
 85 from the World Ocean Atlas 2013 [11, 15]. Red and blue arrows schematically show flows of the warm and cold
 86 waters, respectively. GS is Greenland Sea, IP is Iceland Plateau, NS is Norwegian Sea, EGC is East Greenland
 87 Current, IC is Irminger Current, SG (IG) is Subpolar (Irminger) Gyre, LS is Labrador Sea, NAC is North Atlantic
 88 Current.

89 Chronology of the core has been established from the four AMS ^{14}C - datings of the planktic
 90 foraminifera *Neogloboquadrina (N.) pachyderma* (sin.) shells in the Leibniz Laboratory for Radiometric
 91 Dating and Stable Isotope Research at the Christian-Albrechts-University of Kiel, Germany (Table 1).

92 **Table 1.** List of the accelerator mass spectrometer ^{14}C - datings of the absolute age of the sediment core
 93 AMK-340. Conversion of ^{14}C - datings to the calendar ages was made according [16].

Depth in core	^{14}C - datings, years	Calendar age, years	Dating code
118 cm	5480±50	5767	KIA4187
181 cm	8030±60	8902	KIA4188
260 cm	9220±60	10397	KIA4189
356 cm	11830±70	13600	KIA4190

94 Radiocarbon ages were converted to the calendar ones by the calibration program CALIB 7.1
 95 using MARINE13 scale (standard reservoir age correction R is 405 years with ΔR of 85±79 years) [16].
 96 Age-depth plot is presented in Figure 2. The core AMK-340 spans from ca. 5.7 to ca. 14.5 ka, which is
 97 the mid-Holocene and the end of the last glacial period including most part of the Bølling-Allerød
 98 (BA) warming, and Younger Dryas (YD) cooling. To identify the above-mentioned paleoclimatic
 99 intervals, we have used the standard ages of the Greenland stadials and interstadials from the
 100 INTIMATE event stratigraphy [17]: start of the BA is at ca. 14.7 ka, start of the YD is at ca. 12.9 ka,
 101 and start of the Holocene is at ca. 11.7 ka. Average sedimentation rate of the core is $\approx 26 \text{ cm} \cdot \text{ky}^{-1}$. The
 102 planktic foraminiferal species *N. pachyderma* (sin.) and *Globigerina (G.) bulloides* tests were picked out
 103 for the oxygen and carbon isotopic analysis in the Marine Stable Isotope Lab (MASTIL) of the
 104 National Centre of Antarctic and Ocean Research, Vasco-da-Gama, Goa, India. The size range of the
 105 planktic foraminiferal tests chosen is $>100 \mu\text{m}$. The external precisions of $\delta^{18}\text{O}$ and $\delta^{13}\text{C}$ analysis are
 106 $\pm 0.15\text{‰}$ and $\pm 0.09\text{‰}$, respectively (1σ standard deviation) obtained by repeatedly running NBS-19 as
 107 the Standard ($n=33$). The $\delta^{18}\text{O}$ and $\delta^{13}\text{C}$ values are reported with respect to V-PDB.



108

109 **Figure 2.** Age-depth plot for the core AMK-340 based on the AMS ^{14}C -datings converted to the calendar ages
 110 (black squares). Sedimentation rates are displayed.

111 We studied the marine microfossils (polycystine radiolarians as siliceous microorganisms, and
 112 benthic and planktic foraminifera as calcareous microorganisms) in 37 sediment samples of 2-cm
 113 thickness throughout the core with the best time resolution of 133 years. The interpretation of the
 114 microfossil data will be focused on the interval between 14.5 and 8 ka when the major paleoclimatic

115 changes occurred within the transition between conditions of the last glacial time and recent
116 Holocene interglacial state.

117 For the radiolarian analysis, air-dried sediment samples of 1-2 g were boiled in a solution of
118 30% hydrogen peroxide and sodium pyrophosphate, and the carbonates were removed by adding
119 solution of 10% hydrochloric acid. The residue was washed through a 50 μ m sieve, and then limited
120 part of the washed fraction was settled on the cover glass and mounted on the slide in Canada
121 balsam. As a rule, at least 250-300 radiolarians tests were counted under the transmitted light
122 microscope at the x300-600 magnification.

123 For the foraminiferal analysis, air-dried sediment samples of available weight were washed
124 through 100 μ m sieve, and then numbers of the benthic and planktic species, and mineral grains
125 were counted.

126 The sea paleotemperature was reconstructed by a method of Q-mode factor analysis and
127 transfer functions. A PaleoTool Box software with its latest PC-version [8] provides complete
128 facilities to make a statistical environmental analysis of the micropaleontological data and to
129 estimate conditions of the marine paleohabitat.

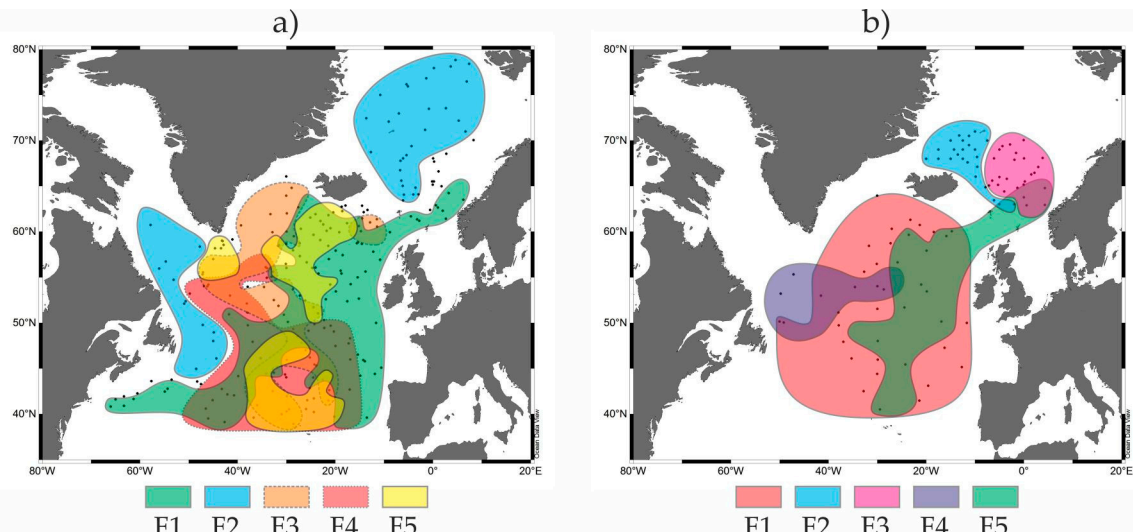
130 Transfer functions which allow paleotemperature estimates are based on the treatment of the
131 modern micropaleontological datasets. The North Atlantic reference datasets on the microfossils in
132 our study are counts of (1) 36 polycystine radiolarian species in 91 bottom surface sediment samples
133 from the area between 40 and 73°N [18], and (2) 23 planktic foraminiferal species in 237 bottom
134 surface sediment samples from the area between 40 and 80°N as a compilation from the Atlantic
135 Ocean database of the Shirshov Institute of Oceanology, Moscow, Russia (134 stations from [19]) and
136 World Ocean database (103 stations from [20]. Stations are presented in Figure 3. Limitations to the
137 construction of modern datasets are described in details by Matul and Mohan [18] regarding the
138 radiolarians study but they also can be applied to the planktic foraminifera. The southern boundary
139 of stations in our datasets is approximately 40°N because, north of this latitude, the North Atlantic
140 was an area of the extremely pronounced environmental changes associated with movements of the
141 Subpolar Front during the Late Quaternary glacials [e.g., 21]. We used the micropaleontological
142 information from those stations which were sampled before 1980th, i.e., before an instability of the
143 North Atlantic thermohaline circulation increased [22]. Thus, our dataset, containing an averaged

144 environmental (climatic) signal, may not be affected by the significant short-term intra-decadal
 145 hydrological changes within the last decades. A temperature at the subsurface depth of 100 m is
 146 chosen as a basic parameter for the interpretation because this depth can be a median level of the
 147 prevailed habitat of radiolarians [23] and planktic foraminifera [24]. In the North Atlantic, the
 148 highest abundances of the marine microzooplankton were found during May-September [25-26],
 149 and we operate with summer temperature. The World Ocean Atlas 2013 [11] provides data on the
 150 modern summer temperature in the North Atlantic and Nordic Seas averaged for 1955-1964.

151 **3. Results and Discussion**

152 *3.1. Modern distribution of the radiolarian and planktic foraminiferal factors (= assemblages) as a base for the*
 153 *paleotemperature estimates*

154 Factor analysis revealed 5 Factors in the modern distribution of both planktic foraminifera and
 155 radiolarians (Figure 3). They describe main oceanographic provinces within the studied area.



156
 157 **Figure 3.** Generalized areas of Factors (≈ assemblages): a) planktic foraminifera (PF) (this study), b)
 158 radiolarians (R) (modified from [18] with simplification) in the bottom surface sediments of the North Atlantic.
 159 F1 is Factor 1 with loadings >0.6 and >0.8 for PF and R, respectively, F2 is Factor 2 with loadings <-0.9 and >0.9
 160 for both PF and R, respectively, F3 is Factor 3 with loadings >0.5 for both PF and R, F4 is Factor 4 with loadings
 161 >0.4 for both PF and R, F5 is Factor 5 with loadings >0.1 for both PF and R.

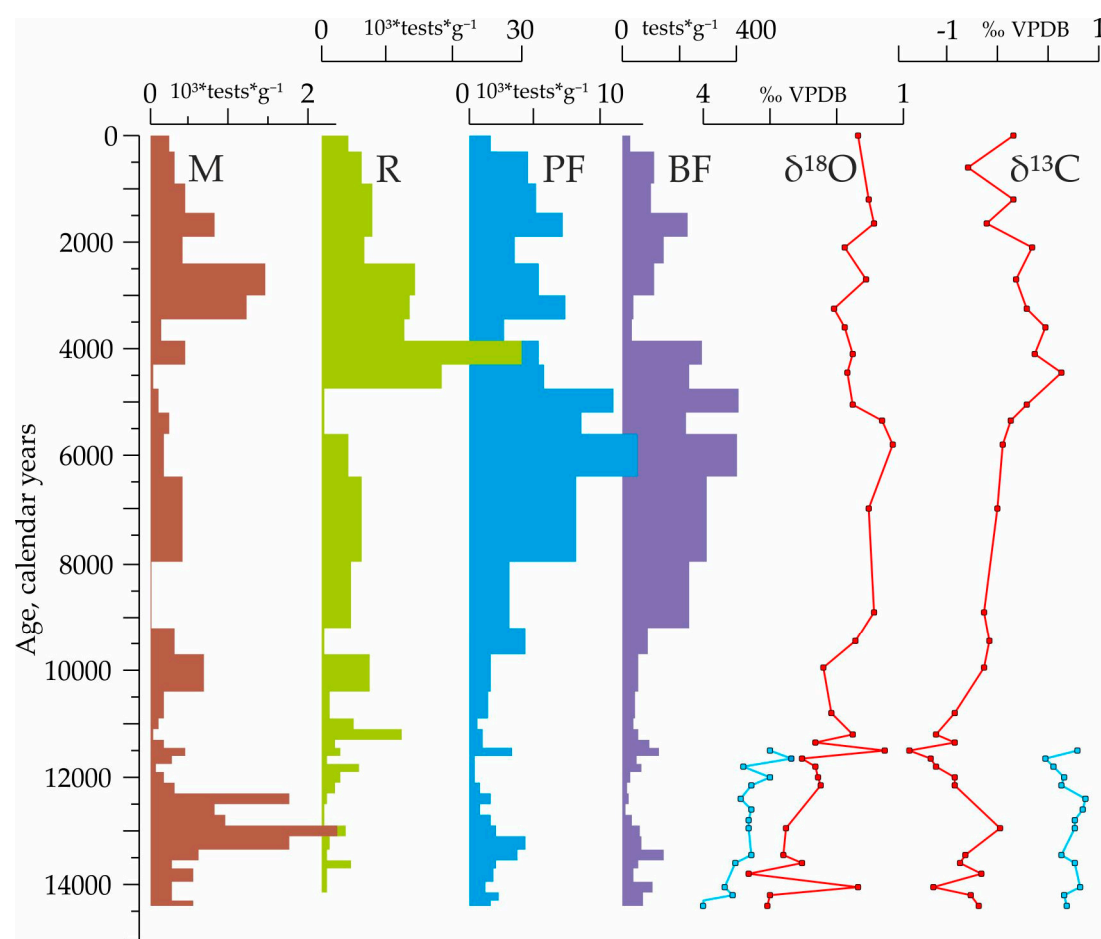
162 Cold-water end-member is Factor 2, with a leading foraminiferal species *N. pachyderma* (sin.)
 163 and radiolarian species *Amphimelissa (A.) setosa*. Foraminiferal assemblages, belonging to Factor 2,

164 are typical for Greenland, Iceland, western and northern Norwegian, and Labrador Sea. Similarly,
165 radiolarian assemblages of Factor 2 occur in the southern Greenland and Iceland Seas but not in the
166 Labrador Sea. The Polar/Arctic waters occupy these areas contacting with branches of the warmer
167 Atlantic waters. Temperate-water Factor 1 lies within the boreal open North Atlantic, where the
168 dominant species are foraminiferal *N. pachyderma* (dex.) and radiolarian *Lithelius (L.) spiralis/minor*
169 group. Other factors give an additional view on the regional patterns of the microfauna in the open
170 North Atlantic. Foraminiferal Factors 3, 4, and 5 are distributed in the western, southern to
171 southwestern, and central parts of the North Atlantic between latitudes of 40 and 65°N with leading
172 species *Turborotalia quinqueloba*, *G. bulloides*, and *Globigerinita glutinata*, respectively. Radiolarian
173 Factors 4 (dominated by *Artostrobium tumidulum* and *Phorticium clevei*) and 5 (dominated by
174 *Lithomelissa setosa* and *Stylodictya validispina*) indicate the mixing waters of the Labrador Sea and
175 western North Atlantic, and eastern North Atlantic, respectively. Radiolarian Factor 3 (dominated
176 by *Pseudodictyophimus gracilipes* and *Actinomma boreale/A. leptoderma* group) is typical for the southern
177 Norwegian Sea, an area of the active interaction of the warmer Atlantic and colder Arctic waters; it
178 has no counter partner in the foraminiferal distribution.

179 Patterns in the distribution of Factors (= microfaunal assemblages) clearly reflect the
180 biogeographic realms of the open North Atlantic and Nordic Seas inferred from different groups of
181 the marine animals and plants [27], radiolarians [28], and planktic foraminifera [29, and references
182 therein]. We present here only generalized areas of the factors as details both on factors and typical
183 species distribution were described in [e.g., 30] for planktic foraminifera, and in [18, 31] for
184 radiolarians. For our purposes it is important to fix that the microfaunal assemblages are closely
185 related to the different environments associated with the cold Polar/Arctic (the Nordic and Labrador
186 Seas with temperatures of 0-5°C on 100-m depth level) and warm temperate (the open North
187 Atlantic with temperatures of 8-15°C on 100-m depth level) water masses. This conclusion gives us a
188 possibility to estimate, based on the transfer functions, the paleotemperature shifts at the principal
189 climatic transitions like the sharp global warming (Termination I) between the last glacial maximum
190 21 ka and the Holocene as recent interglacial time (start at 11.7 ka) when the temperatures on
191 sea-surface in the high latitudes and air temperatures in Greenland could increase at least on 3-6°C
192 and 15°C, respectively [32].

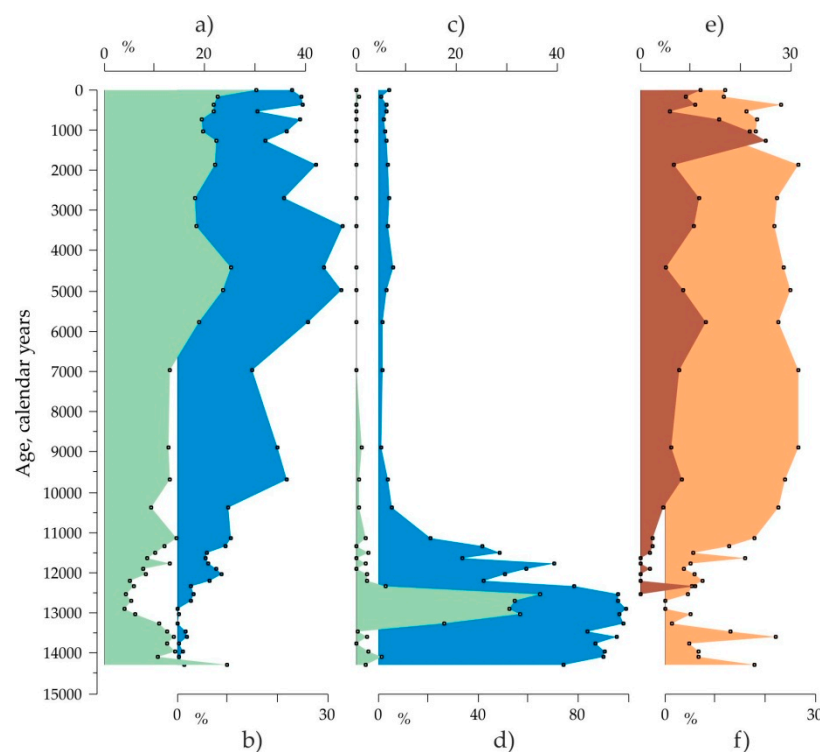
193 3.2. Main indications of the warm and cold-water events in the down-core records covering Termination I
 194 14.5-11.7 ka.

195 The most prominent warming event within the Termination I (BA), and the following cold YD
 196 event as a return to the quasi-glacial state had a weak reflection in the records of the total
 197 microfaunal abundances (Figure 4). Associated changes in the accumulation of radiolarians and
 198 planktic/benthic foraminifera were subtle with small peaks during the BA and stable low values
 199 during the YD.



200
 201 **Figure 4.** Main initial micropaleontological and isotopic data on the core AMK-340. M is a number of the
 202 mineral grains in the sediment fraction >100 μ m calculated per 1 g of dry bulk sediment. R, PF and BF are total
 203 abundances of radiolarians, planktic and benthic foraminifera, respectively, calculated per 1 g of dry bulk
 204 sediment. $\delta^{18}\text{O}$ and $\delta^{13}\text{C}$ were measured in the shells of the planktic foraminifera *G. bulloides* (red line) and *N.*
 205 *pachyderma sin.* (blue line).

206 The response of the main species characterizing the microfossil factors on the paleoclimatic
 207 changes within the BA and YD was different (Figure 5). The boreal radiolarian indicator *L.*
 208 *spiralis/minor* group had high abundances comparable to the modern ones during the BA warming,
 209 then decreased in numbers during the cold YD before reaching its typical percentages at the
 210 beginning of the Holocene (Figure 5a). Similar changes can be recognized in the distribution of the
 211 benthic foraminifera *Cassidulina (C.) teretis* which feed on the bacterias from the soft, enriched by the
 212 organic matter sediments [33]. In contrast, the polar species *N. pachyderma* (sin.) permanently
 213 dominated (40 to 100%) the planktic foraminiferal assemblages both during the warm BA and cold
 214 YD indicating the persistent cold-water conditions on the subsurface depths. But the radiolarian
 215 species *A. setosa*, which is typical for cold-water Greenland and Iceland Seas [31], had a very
 216 prominent peak just at the final part of the BA and earlier part of the YD ca. 13.2-12.3 ka up to 40%
 217 being rare or absent before and after.



218
 219 **Figure 5.** Down-core distribution of the main radiolarian, planktic and benthic foraminiferal species. Temperate
 220 North Atlantic species: a) radiolarian *L. spiralis/minor* group, and b) planktic foraminifera *N. pachyderma* dex.
 221 Subpolar/Polar species: c) radiolarian *A. setosa*, and d) planktic foraminifera *N. pachyderma* sin. Benthic
 222 foraminiferas: e) *G. subglobosa* as marker of spring phytodetrital fluxes [34], and f) *C. teretis* as dweller in soft
 223 surface sediment, rich on bacterias, being abundant during the summer [33].

224 We may suppose that a specific oceanographic situation existed on the Reykjanes Ridge during
225 this 1-ky long time as high percentages of *A. setosa* in the Nordic Seas mark environments of the
226 active mixing of cold (down to ca. -2°C), relatively refreshed Arctic/Polar waters and warmer saline
227 North Atlantic water [35]. Together with *A. setosa*, a significant increase in the abundances of the
228 mineral grains in the sediment fraction of >100 µm marks interval of the YD (Figure 4). Probably, this
229 can be an indication of the Heinrich-like event H-0 as a massive accumulation of the ice-rafted
230 sediment material on the bottom of the northwestern Atlantic Ocean occurred during the YD [36].
231 Andrews [37] proposed the Hudson Bay as a source area for the ice-rafted sediments. However, high
232 abundances of the Greenland cold-water radiolarian species *A. setosa*, which is rare now in the
233 Labrador Sea, could point on the southern Nordic Seas to be main origin place of the ice-rafting
234 within the YD on the Reykjanes Ridge.

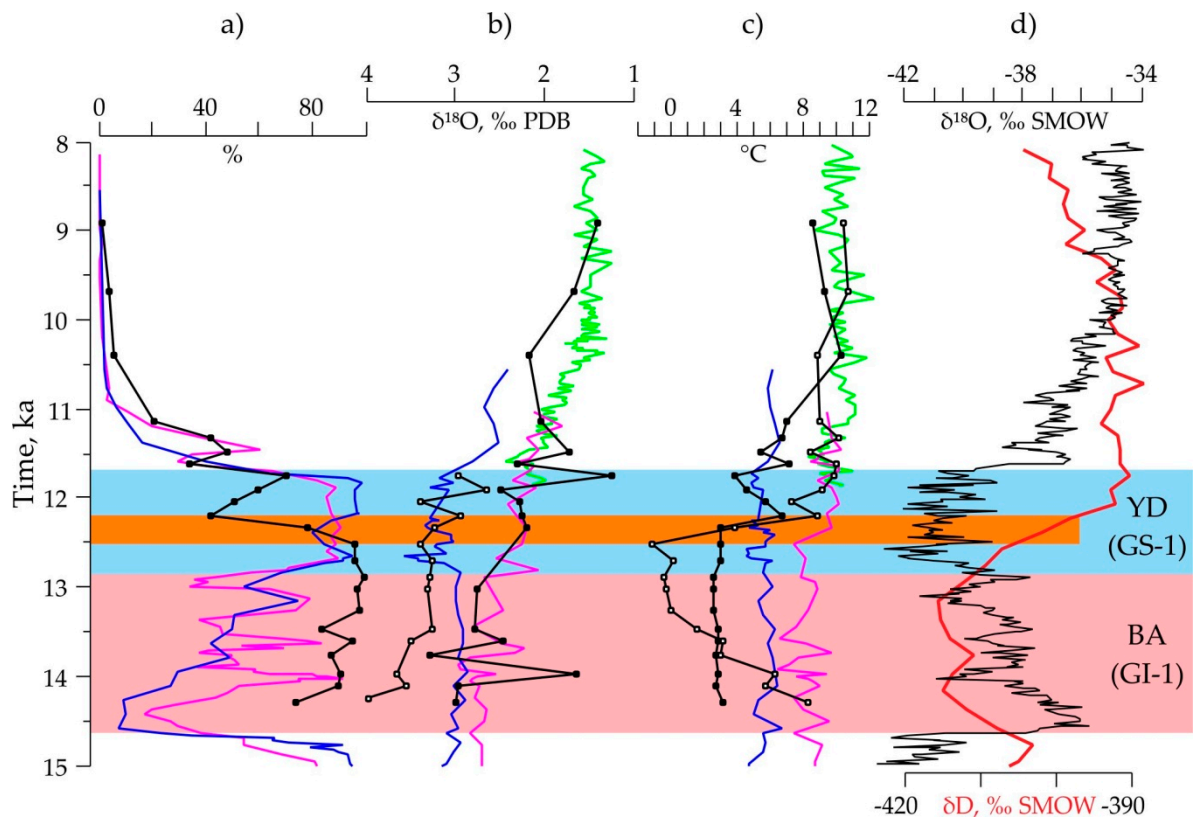
235 The final transition toward the recent interglacial state occurred coincidentally in all
236 micropaleontological records of the core AMK-340 at the end of the YD. But the first changes
237 indicating the warming started in the middle YD chronozone just after time level of 12.5 ka (Figure
238 5). For example, the indicator of the open North Atlantic waters, planktic foraminiferal species *N.*
239 *pachyderma* (dex.), and benthic foraminiferal species *G. subglobosa* as a marker of high phytodetrital
240 fluxes [34] significantly increased percentages or even appeared (in the latter case) from this level.
241 Thus, according to our data on the distribution of the microfossils, the final half of the YD might be
242 an interval of the progressed warming on the Reykjanes Ridge at the latitude of ca. 60°N.

243 The oxygen isotopic signal $\delta^{18}\text{O}$ in the planktic foraminiferal shells of both *N. pachyderma* (sin.)
244 and *G. bulloides* exhibits rather monotonous shift (with short deviations) to the "lighter" values from
245 14.5 to ca. 11 ka (Figure 6). Time interval of 8 to 5.5 ka with lower $\delta^{18}\text{O}$ values of 1.5-1 ‰ (Figure 4)
246 can represent a thermal optimum of the middle Holocene within the Atlantic chronozone [38]. This
247 is supported by the prominent peak of the elevated total abundances of the planktic and benthic
248 foraminifera. We are aware that the $\delta^{18}\text{O}$ changes can't act as a conclusive paleotemperature index
249 because $\delta^{18}\text{O}$ of the foraminiferal shells reflect the $\delta^{18}\text{O}$ of sea water as well governed predominantly
250 by ice volume change on land [39]. Nevertheless, both the temperature increase and hence lesser
251 ice-volume will lower the $\delta^{18}\text{O}$ values, which we observe during 8-5.5 ka. Interpretation of the $\delta^{13}\text{C}$
252 signal in the planktic foraminiferal shells is more complicated. It is under the influence of the

253 photosynthesis vs respiration ratio in the surface to subsurface waters, $\delta^{13}\text{C}$ of the dissolved
254 inorganic carbon, carbonate system parameters, and also temperature [39-40]. Temperature though
255 has a very small effect on the $\delta^{13}\text{C}$ values with a slope of 0.1‰ increase per degree Celsius decrease
256 in temperature [39]. Though, it is advisable to use $\delta^{13}\text{C}$ variability in combination with other proxies.
257 In our study, $\delta^{13}\text{C}$ of *G. bulloides* increases from early Holocene to mid-Holocene and declines
258 slightly thereafter (Figure 4). The total abundances of radiolarians, planktic and benthic foraminifera
259 also show a similar variability (Figure 4). The abundance of benthic foraminiferal species *G.*
260 *subglobosa* – marker of spring phydetrital fluxes, and *C. teretis* – inhabits surface sediments rich on
261 bacterias, also increase during the Holocene (Figure 5). During BA warming, the $\delta^{13}\text{C}$ values as well
262 as the abundances of planktic and benthic foraminifera, and percentages of benthic foraminifera *C.*
263 *teretis* increase slightly. Thus, we infer that the $\delta^{13}\text{C}$ values of planktic foraminifera *G. bulloides* reflect
264 the increased photosynthetic activity during the warm periods.

265 3.3. Paleotemperature estimates for the core AMK-340 and correlation with other paleoclimatic archives.

266 As discussed in the previous subsection, a reaction of the radiolarian and foraminiferal
267 assemblages from the core AMK-340 on the paleoceanographic oscillations during the Termination I
268 was not concurrent. Our micropaleontological records do not coincide in details with the
269 conventional warmings and coolings, the Greenland Stadials and Interstadials [17], at the transition
270 to the Holocene. Reconstructions of the paleotemperature for 100-m water depth (Figure 6) are also
271 not fully coherent with standard oxygen isotopic archives of the Greenland ice cores [41].



272

273 **Fig. 6.** Summer paleotemperature for the water depth of 100 m in the core AMK-340 vs other paleoclimatic data:
 274 a) down-core distribution of the polar planktic foraminifera *N. pachyderma* sin. in the cores AMK-340, black line
 275 with black dots [this study], RAPiD10-1P, blue line, RAPiD-12-1K, green line, and RAPiD15-1P, purple line
 276 [13-14]; b) oxygen isotopic curves for the cores AMK-340, black line with solid black dots based on *G. bulloides*
 277 shells and black line with open dots based on *N. pachyderma* sin. shells [this study], RAPiD10-1P, blue line based
 278 on *N. pachyderma* sin. shells, RAPiD-12-1K, green line based on *G. bulloides* shells, and RAPiD15-1P, purple line
 279 based on *G. bulloides* shells [13-14]; c) paleotemperature for the cores AMK-340, black line with solid black dots
 280 based on the planktic foraminifera and black line with open dots based on the radiolarians (this study),
 281 RAPiD10-1P, blue line based on Mg/Ca in *N. pachyderma* sin. shells, RAPiD-12-1K, green line based on Mg/Ca in
 282 *G. bulloides* shells, and RAPiD15-1P, purple line based on Mg/Ca in *G. bulloides* shells [13-14]; d) oxygen isotopic
 283 curve for the Greenland NGRIP ice core, black line [41], and deuterium curve for the Antarctic EPICA ice core
 284 [42]. Light-blue stripe is an interval of the cold YD (Greenland Stadial GS-1), rose stripe is an interval of the
 285 warm BA (Greenland Interstadial GI-1), and light-brown stripe is a transition to the warmer conditions [this
 286 study] within the conventional cold YD.

287 The foraminiferal temperature had monotonous, low values of 2-3°C from 14.5 to ca. 12.2 ka,
288 and then it started to increase, with some fluctuations, up to 8-10°C at the beginning of Holocene.
289 Low but weakly variable foraminiferal temperature could arise from the stable dominance of the
290 polar species *N. pachyderma* (sin.). The monospecific (*N. pachyderma* (sin.)) planktic foraminiferal
291 assemblages now are distributed in the cold-water Labrador and Seas within the wide range of
292 summer sea-surface temperatures of 6 to -2°C [43] or, in our database, summer temperature at 100 m
293 depth of 3 to -1°C. It could be that the statistical program of the paleotemperature calculations,
294 operating with *N. pachyderma* (sin.) dominance, may not provide the proper values from this
295 temperature range.

296 The radiolarian paleotemperature at the BA start, in contrast to the foraminiferal one, exhibits
297 high values of about 8°C being comparable with modern and Holocene numbers in the area. It
298 dropped steadily toward the BA end, and was very low of 0 to -2°C from ca. 13.5 to 12.5 ka, i.e., just
299 until the middle YD cold interval.

300 The next warming step after the BA, as documented both by the radiolarian and foraminiferal
301 temperatures, occurred in the area of core AMK-340 12.5-12.2 ka (Figure 6) or considerably earlier
302 than the Holocene started. Neither oxygen isotopic records nor sea-surface paleotemperature
303 estimates on Mg/Ca in the planktic foraminifera, and percentages of the polar *N. pachyderma* (sin.)
304 from the North Atlantic cores south of Iceland [13-14] fixed such event. But some other studies can
305 support our results. Pearce et al. [44] found the start of the pre-Holocene warming at the time level of
306 12.2 ka based on the diatom study of the sediment core south of Newfoundland. They concluded the
307 evident difference of the early to late YD local paleoceanography. Ebbesen and Hald [45] reported
308 similar results on the cold YD before 12.5 ka and warmer conditions after this level in the Norwegian
309 Sea. We may see a good visual correlation of this warming step with a sharp change from lower to
310 higher δD values in the Antarctic EPICA ice-core records [42]. This can allow us to suspect in our
311 records of the subsurface paleotemperature a teleconnection to the paleoclimatic changes in the
312 Southern Hemisphere which was proposed, e.g., by Rickaby and Elderfield [46] for the coolings
313 during the pre-BA Heinrich-1 event and YD, and by Barker et al. [47] for some abrupt paleoclimatic
314 events during the last deglaciation.

315 **4. Conclusions.**

316 The North Atlantic areas of the radiolarian and planktic foraminiferal assemblages or main
317 factors, as defined by the Q-mode analysis of the PanTool Box software, match together in their
318 general outlines and reflect a regional biogeography, distribution and interaction of the major cold-
319 and warm-water masses. However, there is a dissimilarity possibly arising from the specific habitat
320 of different radiolarian and foraminiferal species.

321 The response of the main microfossil species on the paleoceanographic changes within the
322 transition from the BA warming BA through the cold YD to the warm Holocene was different. The
323 BA warming was well reflected in the radiolarian and benthic but not planktic foraminiferal record.
324 The cold-water radiolarian species *A. setosa* as the Greenland Sea indicator is, probably, alone to
325 mark cooling at the end of the BA and within the start of the YD event 13.2-12.3 ka. Our
326 micropaleontological and isotopic data along with the paleotemperature estimates for the Reykjanes
327 Ridge at ca. 60°N document that, after the warm BA, the middle YD ca. 12.5-12.2 ka is the next
328 significant step toward the Holocene warming. Probably, the paleoceanographic changes in the area
329 of study during the global warming within the Termination I occurred on the subsurface depths
330 earlier than on the sea surface.

331 **Author Contributions:** Conceptualization, Alexander Matul; Methodology, Alexander Matul, Max S. Barash,
332 and Manish Tiwari; Investigation, Alexander Matul, Max S. Barash, Tatyana A. Khusid, Padmasini Behera, and
333 Manish Tiwari; Writing – Original Draft Preparation, Alexander Matul, and Manish Tiwari; Writing – Review &
334 Editing, Alexander Matul, and Manish Tiwari.

335 **Funding:** This research was funded the Russian Science Foundation and Department of Science and
336 Technology of the Ministry of Science and Technology of India, Joint Project No. 16-47-02009. The funds for the
337 same were extended by National Centre for Antarctic and Ocean Research (NCAOR), Goa, Ministry of Earth
338 Sciences. Funding of the work on the initial micropaleontological data was from the Russian Agency of the
339 Scientific Organization, Project № 0149-2018-0016 for the Shirshov Institute of Oceanology, Moscow, Russia.

340 **Acknowledgments:** The authors are grateful for support from the Russian Government, the Russian Science
341 Foundation and the Administration of Shirshov Institute of Oceanology. MT and PB would like to thank the

342 Secretary, Ministry of Earth Sciences, Govt. of India and the Director, National Centre for Antarctic and Ocean
343 Research for extending support to this project (NCAOR Contribution No. XX/XXXX). The authors thank Dr.
344 R.F. Spielhagen, GEOMAR Helmholtz Centre for Ocean Research, Kiel, Germany, and Dr. H. Erlenkeuser, The
345 Leibniz Laboratory for Radiometric Dating and Stable Isotope Research, Christian-Albrechts-University of Kiel,
346 Germany, for providing of the ¹⁴C-datings.

347 **Conflicts of Interest:** The authors declare no conflict of interest. The founding sponsors had no role in the
348 design of the study; in the collection, analyses, or interpretation of data; in the writing of the manuscript, and in
349 the decision to publish the results.

350 References

- 351 1. Delworth, T.L.; Zeng, F. The Impact of the North Atlantic Oscillation on Climate through Its Influence
352 on the Atlantic Meridional Overturning Circulation. *J. Climate* **2016**, *29*, 9412-962. DOI:
353 10.1175/JCLI-D-15-0396.1.
- 354 2. Löfverström, M.; Lora, J.M. Abrupt regime shifts in the North Atlantic atmospheric circulation over the
355 last deglaciation. *Geophys. Res. Lett.* **2017**, *44*, 8047-8055. DOI:10.1002/2017GL074274.
- 356 3. Knorr, G.; Lohmann, G. Rapid transitions in the Atlantic thermohaline circulation triggered by global
357 warming and meltwater during the last deglaciation. *Geochem. Geophys. Geosyst.* **2007**, *8*, Q12006: 22.
358 DOI:10.1029/2007GC001604.
- 359 4. Overpeck, J.T.; Peterson, L.C.; Kipp, N.; Rind, D. Climate change in the circum-North Atlantic region
360 during the last deglaciation. *Nature* **1989**, *338*, 553-557. DOI:10.1038/338553a0.
- 361 5. Bauch, H.A.; Kandiano, E.S.; Helmke, J.P. Contrasting ocean changes between the subpolar and polar
362 North Atlantic during the past 135 ka. *Geophys. Res. Lett.* **2012**, *39*, L11604: 7.
363 DOI:10.1029/2012GL051800.
- 364 6. Matul, A.G. On the problem of paleoceanological evolution of the Reykjanes ridge region (North
365 Atlantic) during the last deglaciation based on a study of radiolaria. *Oceanology* **1995**, *34*, 806-814.
- 366 7. Matul, A.G.; Yushina, I.G. Radiolarians in North Atlantic sediments. *Ber. Polarforsch.* **1999**, *306*, 35-45.
- 367 8. Sieger, R.; Grobe, H. PanTool – a Swiss Army Knife for data conversion and recalculation. *PANGAEA*:
368 Alfred Wegener Institute, Helmholtz Center for Polar and Marine Research (AWI), Bremerhaven,

369 Center for Marine Environmental Sciences, University Bremen (MARUM), Bremen, Germany, 2012.

370 Available online: <https://doi.org/10.1594/PANGAEA.787549> (accessed on 31 July 2018).

371 9. Krauss, W. Currents and mixing in the Irminger Sea and in the Iceland Basin. *J. Geophys. Res.* **1995**,

372 100(C6), 10,851-10,871.

373 10. Våge, K.; Pickart, R.S.; Sarafanov, A.; Knutsen, Ø.; Mercier, H.; Lherminier, P.; van Aken, H.M.;

374 Meincke, J.; Quadfasel, D.; Bacon, S. The Irminger Gyre: Circulation, convection, and interannual

375 variability. *Deep-Sea Research I* **2011**, 58, 590-614. DOI:10.1016/j.dsr.2011.03.001.

376 11. Locarnini, R.A.; Mishonov, A.V.; Antonov, J.I.; Boyer, T.P.; Garcia, H.E.; Baranova, O.K.; Zweng, M.M.;

377 Paver, C.R.; Reagan, J.R.; Johnson, D.R.; et al. World Ocean Atlas 2013. NOAA, U.S. Department of

378 Commerce: Washington, DC, USA, 2013; NOAA Atlas NESDIS 73, Volume 1: Temperature. Available

379 online: <https://www.nodc.noaa.gov/OC5/woa13> (accessed on 31 July 2018).

380 12. Weinelt, M.; Vogelsang, E.; Kucera, M.; Pflaumann, U.; Sarnthein, M.; Voelker, A.; Erlenkeuser, H.;

381 Malmgren, B.A. Variability of North Atlantic heat transfer during MIS 2. *Paleoceanography* **2003**, 18,

382 1071: 18. DOI:10.1029/2002PA000772.

383 13. Thornalley, D.J.R.; McCave, I.N.; Elderfield, H. Freshwater input and abrupt deglacial climate change

384 in the North Atlantic. *Paleoceanography* **2010**, 25, PA1201. DOI:10.1029/2009PA001772.

385 14. Thornalley, D.J.R.; Elderfield, H.; McCave, I.N. Reconstructing North Atlantic deglacial surface

386 hydrography and its link to the Atlantic overturning circulation. *Global Planet. Change* **2011**, 79, 163-175.

387 DOI: 10.1016/j.gloplacha.2010.06.003.

388 15. Zweng, M.M.; Reagan, J.R.; Antonov, J.I.; Locarnini, R.A.; Mishonov, A.V.; Boyer, T.P.; Garcia, H.E.;

389 Baranova, O.K.; Johnson, D.R.; Seidov, D.; Biddle, M.M. World Ocean Atlas 2013.NOAA, U.S.

390 Department of Commerce: Washington, DC, USA, 2013; NOAA Atlas NESDIS 74, Volume 2: Salinity.

391 Available online: <https://www.nodc.noaa.gov/OC5/woa13> (accessed on 31 July 2018).

392 16. Stuiver, M.; Reimer, P.J.; Reimer, R.W., CALIB 7.1 [WWW program], 2018. Available online:

393 <http://calib.org> (accessed on 31 July 2018).

394 17. Rasmussen, S.O.; Bigler, M.; Blockley, S.P.; Blunier, T.; Buchardt, S.L.; Clausen, H.B.; Cvijanovic, I.;

395 Dahl-Jensen, D.; Johnsen, S.J.; Fischer, H.; et al. A stratigraphic framework for abrupt climatic changes

396 during the Last Glacial period based on three synchronized Greenland ice-core records: refining and

397 extending the INTIMATE event stratigraphy. *Quaternary Sci. Rev.* **2014**, *106*, 14–28.
398 <http://dx.doi.org/10.1016/j.quascirev.2014.09.007>.

399 18. Matul, A.; Mohan, R. Distribution of Polycystine Radiolarians in Bottom Surface Sediments and Its
400 Relation to Summer Sea Temperature in the High-Latitude North Atlantic. *Front. Mar. Sci.* **2017**, *4*, 330:
401 1–330; DOI:10.3389/fmars.2017.00330.

402 19. Barash, M.S. Fossil Plankton Stratigraphies. NOAA/NGDC Paleoclimatology Program: Boulder, CO,
403 USA, 1993; IGBP PAGES/World Data Center-A for Paleoclimatology Data Contribution Series # 93-037.
404 Available online:
405 https://www1.ncdc.noaa.gov/pub/data/paleo/paleocean/fossil_plankton/russian_fossil_plankton
406 (accessed on 31 July 2018).

407 20. Pflaumann, U.; Duprat, J.M.; Pujol, C.; Labeyrie, L.D. Distribution of planktic foraminifera in surface
408 sediments of the Atlantic Ocean. 1996. PANGAEA: Alfred Wegener Institute, Helmholtz Center for
409 Polar and Marine Research (AWI), Bremerhaven, Center for Marine Environmental Sciences,
410 University Bremen (MARUM), Bremen, Germany, 1996. Available online:
411 <https://doi.org/10.1594/PANGAEA.51621> (accessed on 31 July 2018).

412 21. Labeyrie, L.; Vidal, L.; Cortijo, E.; Paterne, M.; Arnold, M.; Duplessy, J.C.; Vautravers, M.; Labracherie,
413 M.; Duprat, J.; Turon, J.L.; et al. Surface and Deep Hydrology of the Northern Atlantic Ocean during
414 the past 150 000 Years. *Phil. Trans. R. Soc. Lond. B* **1995**, *348*, 255–264. DOI:10.1098/rstb.1995.0067.

415 22. Stocker, T.F.; Knutti, R.; Plattner, G.-K. The Future of the Thermohaline Circulation – a Perspective. In
416 *The Oceans and Rapid Climate Change: Past, Present, and Future, Geophysical Monograph Series 126*, 1st ed.;
417 Seidov, D., Haupt, B.J., Maslin, M., Eds.; American Geophysical Union: Washington, DC, USA, 2013;
418 pp. 277–293, ISBN 0-87590-985-X.

419 23. Zas'ko, D.N. Quantitative distribution of radiolarians in the North Atlantic plankton. *Oceanology* **2001**,
420 *41*(12), 86–93.

421 24. Rebotim, A.; Voelker, A.H.L.; Jonkers, L.; Waniek, J.J.; Meggers, H.; Schiebel, R.; Fraile, I.; Schulz, M.;
422 Kucera, M. Factors controlling the depth habitat of planktonic foraminifera in the subtropical eastern
423 North Atlantic. *Biogeosciences* **2017**, *14*, 827–859. DOI:10.5194/bg-14-827-2017.

424 25. Colebrook, J.M. Continuous plankton records: seasonal variations in the distribution and abundance
425 of plankton in the North Atlantic Ocean and the North Sea. *J. Plankton Res.* **1982**, *4*, 435–462.

426 26. Parsons, T. R., Takahashi, M., Hargrave, B. *Biological oceanographic processes*, 3rd Edition. Pergamon
427 Press: Oxford, UK, 1984, ISBN 9781483286174.

428 27. Costello, M.J.; Tsai, P.; Wong, P.S.; Cheung, A.K.L.; Basher, Z.; Chaudhary, C. Marine biogeographic
429 realms and species endemism. *Nat. Commun.* **2017**, *8*, 1057: 1-1057: 10.
430 <http://doi.org/10.1038/s41467-017-01121-2>.

431 28. Boltovskoy, D.; Correa, N. Biogeography of Radiolaria Polycystina (Protista) in the World Ocean.
432 *Prog. Oceanogr.* **2016**, *149*, 82-105. DOI:10.1016/j.pocean.2016.09.006.

433 29. Boltovskoy, D. Foraminifers (Planktonic). In *Encyclopedia of Marine Geosciences*; Harff, J., Mesched, M.,
434 Petersen, S., Thiede, J., Eds.; Springer Science+Business Media: Dordrecht, Netherlands, 2014; pp. 1-9,
435 ISBN 978-94-007-6238-1.

436 30. Kipp, N.G. New Transfer Function for Estimating Past Sea-Surface Conditions from Sea-Bed
437 Distribution of Planktonic Foraminiferal Assemblages in the North Atlantic. *Mem. Geol. Soc. Am.* **1976**,
438 *145*, 9-42. DOI:10.1130/MEM145-p3.

439 31. Bjørklund, K.R.; Cortese, G.; Swanberg, N.R.; Schrader, H.J. Radiolarian faunal provinces in surface
440 sediments of the Greenland, Iceland and Norwegian (GIN) Seas. *Mar. Micropaleontol.* **1998**, *35*, 105-140.

441 32. Clark, P.U.; Shakun, J.D.; Baker, P.A.; Bartlein, P.J.; Brewer, S.; Brook, E.; Carlson, A.E.; Cheng, H.;
442 Kaufman, D.S.; Liu, Z.; et al. Global climate evolution during the last deglaciation. *P. Natl. A. Sci. USA*
443 **2012**, *109* (19), E1134-E1142. DOI:10.1073/pnas.1116619109.

444 33. Gooday, A.J.; Lambshead, P.J.D. Influence of seasonally deposited phytodetritus on benthic
445 foraminiferal populations in the bathyal northeast Atlantic: the species response. *Mar. Ecol. Prog. Ser.*
446 **1989**, *58*, 53-67.

447 34. Suhr, S.B.; Pond, D.; Gooday, A.J.; Smith, C.R. Selective feeding by benthic foraminifera on
448 phytodetritus on the western Antarctic Peninsula shelf: evidence from fatty acid biomarker analysis.
449 *Mar. Ecol. Prog. Ser.* **2003**, *262*, 153-162.

450 35. Bjørklund, K.R.; Hatakeyama, K.; Kruglikova, S.B.; Matul, A.G. *Amphimelissa setosa* (Cleve) (Polycystina,
451 Nassellaria) – a stratigraphic and paleoecological marker of migrating polar environments in the
452 northern hemisphere during the Quaternary. *Stratigraphy* **2015**, *12*, 23-37.

453 36. Hillaire-Marcel, C.; de Vernal, A. 2008. Stable isotope clue to episodic sea ice formation in the glacial
454 North Atlantic. *Earth Planet. Sc. Let.* **2008**, *268*, 143-150. <https://doi.org/10.1016/j.epsl.2008.01.012>.

455 37. Andrews, J.; Jennings, A.E.; Kerwin, M.; Kirby, M.; Manley, W.; Miller, G.H.; Bond, G.; MacLean, B. A
456 Heinrich-like event, H-0 (DC-0): Source(s) for detrital carbonate in the North Atlantic during the
457 Younger Dryas Chronozone. *Paleoceanography* **1995**, *10*, 943-952. <https://doi.org/10.1029/95PA01426>.

458 38. Jansen, E.; Andersson, C.; Moros, M.; Nisancioglu, K.H.; Nyland, B.F.; Telford, R.J. The Early to
459 Mid-Holocene Thermal Optimum in the North Atlantic. In *Natural Climate Variability and Global*
460 *Warming: A Holocene Perspective*; Battarbee, R.W., Binney, H.A., Eds. Wiley-Blackwell: Chichester, UK,
461 2008; pp. 123-137, ISBN 9781405159050.

462 39. Ravelo, A.C.; Hillaire-Marcel, C. The Use of Oxygen and Carbon Isotopes of Foraminifera in
463 Paleoceanography. In *Developments in Marine Geology*; Hillaire-Marcel, C., de Vernal, A., Eds.; Elsevier:
464 AE Amsterdam, Netherlands, 2007. Volume 1, Proxies in Late Cenozoic Paleoceanography, pp.
465 735-764. ISBN 978-0-444-52755-4.

466 40. Jonkers, L.; van Heuven, S.; Zahn, R.; Peeters, F.J.C. Seasonal patterns of shell flux, $\delta^{18}\text{O}$ and $\delta^{13}\text{C}$ of
467 small and large *N. pachyderma* (s) and *G. bulloides* in the subpolar North Atlantic. *Paleoceanography*
468 **2013**, *28*, 164-174. DOI: 10.1002/palo.20018.

469 41. NGRIP members. High-resolution record of Northern Hemisphere climate extending into the last
470 interglacial period. *Nature* **2004**, *431*, 147-151. DOI:10.1038/nature02805.

471 42. EPICA community members. Eight glacial cycles from an Antarctic ice core. *Nature* **2004**, *429*, 623-628.
472 DOI:10.1038/nature02599.

473 43. Eynaud, F. Planktonic foraminifera in the Arctic: Potentials and issues regarding modern and
474 Quaternary populations. *IOP C. Ser. Earth Env.* **2011**, *14*, 1-12. DOI:10.1088/1755-1315/14/1/012005.

475 44. Pearce, C.; Seidenkrantz, M.-S.; Kuijpers, A.; Masser, Reynisson, N.F.; Kristiansen, S.M. Ocean lead at
476 the termination of the Younger Dryas cold spell. *Nat. Commun.* **2013**, *4*, 1664: 1-1664: 6.
477 DOI:10.1038/ncomms2686.

478 45. Ebbesen, H.; Hald, M. Unstable Younger Dryas climate in the northeast North Atlantic. *Geology* **2004**,
479 32, 673-676. <https://doi.org/10.1130/G20653.1>.

480 46. Rickaby, R.E.M.; Elderfield, H. Evidence from the high-latitude North Atlantic for variations in
481 Antarctic Intermediate water flow during the last deglaciation. *Geochem. Geophys. Geosyst.* **2005**, *6*,
482 Q05001: 12. DOI:10.1029/2004GC000858.

483 47. Barker, S.; Diz, P.; Vautravers, M.J.; Pike, J.; Knorr, G.; Hall, I.R.; Broecker, W.S. Interhemispheric
484 Atlantic seesaw response during the last deglaciation. *Nature* 2009, **457**, 1097-1102.
485 DOI:10.1038/nature07770.

486 48. Matul, A. Distribution of the polycystine radiolarian species in the Quaternary sediment cores of the
487 subarctic North Atlantic and Sea of Okhotsk. *Data in Brief* 2018, **17**, 438-441.
488 <https://doi.org/10.1016/j.dib.2018.01.041>.